

A FAST EXPANDING H I SHELL IN W44: A PREEXISTING WIND-BLOWN SHELL OVERTAKEN BY A SUPERNOVA REMNANT

BON-CHUL KOO

Department of Astronomy, Seoul National University, Seoul 151-742, Korea

AND

CARL HEILES

Astronomy Department, University of California, Berkeley, CA 94720

Received 1994 March 14; accepted 1994 October 6

ABSTRACT

We confirm from higher resolution observations that the previously detected high-velocity H I gas in W44 is an expanding shell associated with the supernova remnant (SNR). The H I shell is expanding at 150 km s^{-1} and has a kinetic energy of 8×10^{49} ergs, which is very likely to have been imparted by the supernova (SN) explosion that produced W44. However, the radius of the H I shell $R_H \simeq 9$ pc, which is obtained by extrapolating the high-velocity H I data, is considerably smaller than $R_C \simeq 15$ pc of the W44 radio continuum shell. It is possible that the uncertainty associated with our extrapolation has led us to significantly underestimate the size of the H I shell. But if $R_H \simeq R_C \simeq 15$ pc, then the coexistence of the H I shell, the centrally peaked X-ray emission, and the 2×10^4 yr old pulsar PSR 1853+01 in W44 is very difficult to understand based on available theoretical models. Furthermore, there are optical filaments mainly confined within the H I shell.

We therefore propose that the H I and radio continuum shells are physically distinct shells. The double-shell structure may have been produced by a SN explosion inside a preexisting wind bubble. We interpret the inner H I structure as a preexisting wind shell that has been rejuvenated and disrupted by the SN blast wave, and the outer radio continuum structure as a SNR shell composed of newly swept-up ambient medium. The well-separated double-shell structure suggests that the SNR W44 is in the “memory-losing” phase, where the SN blast wave has now obliterated the presence of the wind bubble. We discuss the implications of the double-shell structure on the evolutionary history of W44.

Subject headings: ISM: individual (W44) — radio lines: ISM — supernova remnants

1. INTRODUCTION

Type II and Ib supernovae (SNs) have massive progenitors which blow out stellar winds during their evolution. Stellar winds during the main-sequence lifetime sweep out the ambient interstellar medium to produce hot diffuse bubbles surrounded by dense shells: “wind bubbles” and “wind shells” (Castor, McCray, & Weaver 1975; Weaver et al. 1977). The innermost region of these wind bubbles may be filled with circumstellar material that has been ejected during the late stages of stellar evolution. Most of the SN ejecta produced inside such a diffuse wind bubble expands unimpeded until the blast wave hits the dense wind shell. When the blast wave hits the wind shell, the fraction of the shocked ejecta increases and a shock propagates into the wind shell. It is at this moment that a large shell-type supernova remnant (SNR) appears in X-ray, optical, and radio continuum emission. The above is a scenario for the evolution of Type II and Ib SNRs (Tenorio-Tagle et al. 1990, 1991). According to this, large Type II and Ib shell-type SNRs either are crossing or should have crossed a preexisting wind shell. Braun & Strom (1987) suggested that the Cygnus Loop, where the X-ray and radio emissions extend to a radius 20%–30% larger than the bright optical filamentary shell, is an example of such SNRs. In this paper, we present evidence that the well-known SNR W44 is a more dramatic example of such SNRs.

W44, also known as G34.7–0.4 and 3C 392, is a shell-type SNR in radio continuum (e.g., Kundu & Velusamy 1972; Clark, Green, & Caswell 1975; Kassim 1992). The shell is

somewhat elongated ($30' \times 39'$), and the eastern portion of the SNR shows enhanced radio emission. The VLA map (FWHM = $15''$) recently published by Jones, Smith, & Angelini (1993, hereafter JSA) shows that a large fraction of the radio emission is concentrated in filaments and loops. In X-rays, however, the SNR has a centrally peaked morphology (Smith et al. 1985, hereafter SJWW; JSA; Rho et al. 1994, hereafter RPSH). Most of the X-ray emission is believed to be thermal. RPSH discovered optical filaments within the X-ray-emitting region. At $9'$ to the south from the center, Wolszczan, Cordes, & Dewey (1991) discovered a pulsar, PSR 1853+01, which has a spin-down age of $\sim 2 \times 10^4$ yr. The dispersion measure based distance to the pulsar of 3.2 kpc (Wolszczan et al. 1991) is almost identical to the kinematic distance of 3 kpc to W44 (Caswell et al. 1975; Sato 1986), and the association of the pulsar with the SNR is very likely.

In our previous study (Koo & Heiles 1991), we detected H I gas moving as fast as $\sim +150 \text{ km s}^{-1}$ with respect to the ambient medium around W44 but were not able to resolve its structure using the Hat Creek 26 m telescope (FWHM = $36'$). In this study, we carried out high-resolution H I observations and have found that the high-velocity H I gas in a portion of an expanding shell *within* the radio-emitting region. The dynamical center of the shell is almost identical with the geometrical center of the radio continuum shell. It is the inner region of the H I shell from which most of the X-ray emission comes. The filamentary optical emission detected by RPSH is confined within the H I shell. The morphology strongly sug-

gests that the H I shell is probably a preexisting wind shell reaccelerated by the SN blast wave.

2. OBSERVATIONS

H I 21 cm line observations were made using the telescope (FWHM = 3'.3) at the Arecibo Observatory¹ in 1991 September. Both circular polarizations were observed simultaneously using two 1024 channel correlators, each with a total bandwidth of 5 MHz, so that the velocity resolution was 2.06 km s⁻¹ (after Hanning smoothing). Each spectrum was obtained by integrating 1 minute using frequency switching. A rectan-

gular area bounded by $\alpha_{1950} = 18^{\text{h}}51^{\text{m}}54^{\text{s}}$ to $18^{\text{h}}55^{\text{m}}06^{\text{s}}$ and $\delta_{1950} = +0^{\circ}57'$ to $+01^{\circ}39'$ has been mapped at 3' spacing.

3. RESULTS

Figures 1a and 1b show the high-velocity (HV) H I brightness distribution integrated between $v_{\text{LSR}} = +135$ and $+170$ km s⁻¹. A shell-like structure within the radio-emitting region of W44 is clearly seen in Figure 1a. The dynamical center of the H I shell, defined to be the average position weighted by the integrated intensity between $v_{\text{LSR}} = +130$ and $+200$ km s⁻¹, is $(\alpha_{1950}, \delta_{1950}) = (18^{\text{h}}53^{\text{m}}35^{\text{s}} \pm 2^{\text{s}}, +01^{\circ}17'0 \pm 0.9)$. This dynamical center of the H I shell is almost identical with the geometrical center of the radio continuum shell (Kundu & Velusamy 1974; Clark et al. 1975; Kassim 1992). The positional coincidence almost certainly implies that the fast expanding H I shell is associated with the SNR W44. The

¹ The Arecibo Observatory is part of the National Astronomy and Ionosphere Center, which is operated by Cornell University under contract with the National Science Foundation.

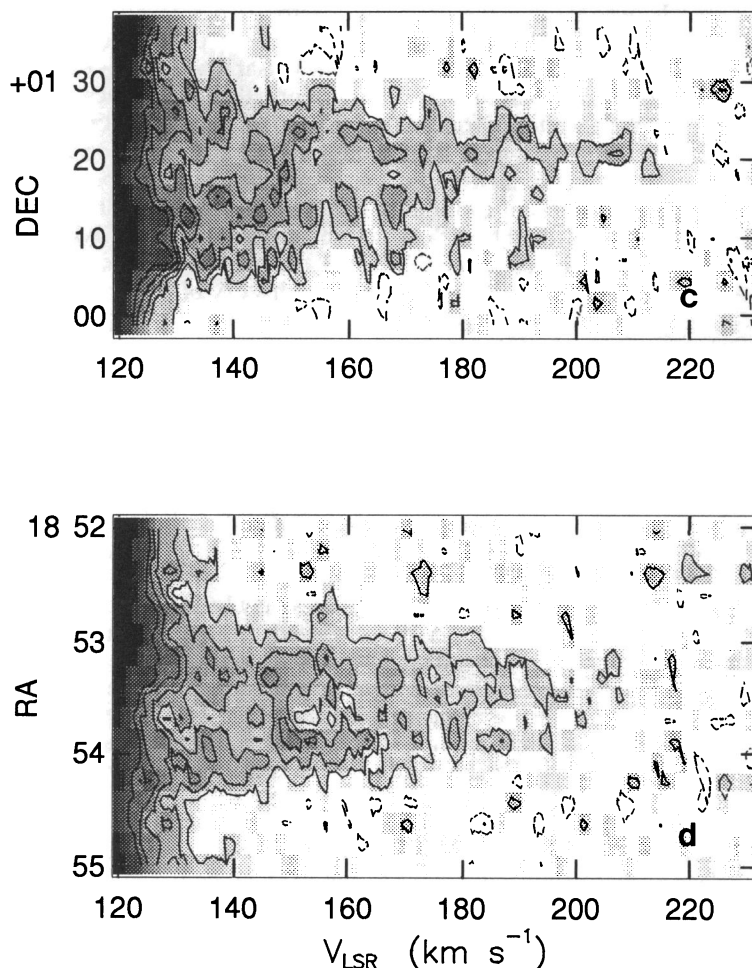
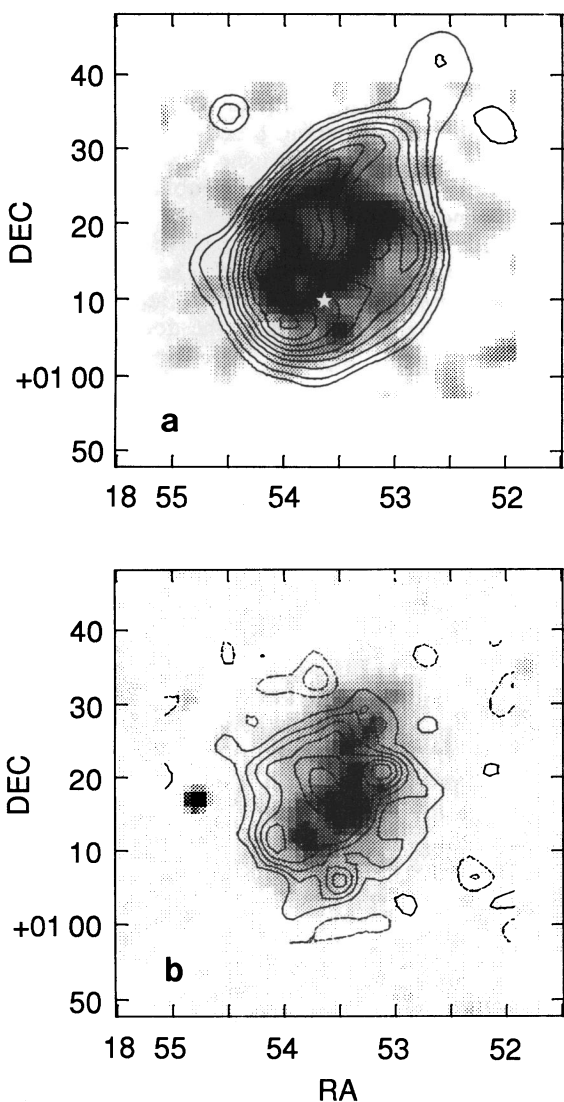


FIG. 1.—(a) High-velocity H I brightness map (gray shades) superposed on the 11 cm radio continuum map (contours) of W44. The H I map is obtained by averaging the emission between $v_{\text{LSR}} = +135$ and $+170$ km s⁻¹. The radio continuum map is obtained from the 11 cm survey of Reich et al. (1990) and the contour levels (in K) are 1, 2, 4, 6, 8, 10, 12, 14, and 16. (b) Same H I map (contours) superposed on the ROSAT X-ray map (gray shades) of W44 (RPSH). Contour levels (in K) increases from -0.1 to $+0.3$ at 0.05 interval. Negative levels are marked by dotted contours. (c) Position-velocity diagram of the high-velocity H I gas along $\alpha_{1950} = 18^{\text{h}}53^{\text{m}}30^{\text{s}}$. Contour levels (in K) increases from -0.1 to $+0.5$ at 0.1 interval. (d) Same as (c) but along $\delta_{1950} = +01^{\circ}18'$.

TABLE 1
PARAMETERS OF THE EXPANDING H I SHELL

Parameter	Estimated Value
Velocity centroid	$(18^{\text{h}}53^{\text{m}}35^{\text{s}} \pm 2^{\text{s}}, +01^{\circ}17'0 \pm 0'9)$
Expansion velocity	$150 \pm 15 \text{ km s}^{-1}$
Radius	9 pc
Mass	$350 M_{\odot}$
Momentum	$5 \times 10^4 M_{\odot} \text{ km s}^{-1}$
Kinetic energy	$8 \times 10^{49} \text{ ergs}$

association is further supported by Figure 1b, which shows that most of the X-ray emission in W44 (RPSH) originates from the inner region of the H I shell. The optical filaments detected by RPSH are also mainly confined within the H I shell.

The velocity structure of the HV H I gas is shown in Figures 1c and 1d, which are the position-velocity diagrams crossing the central portion of W44 along declination and right ascension, respectively. The HV H I emission is discernible between $v_{\text{LSR}} = +125$ and $+210 \text{ km s}^{-1}$. At lower velocities ($-70 \leq v_{\text{LSR}} \leq 125 \text{ km s}^{-1}$), the Galactic background H I emission dominates. At large negative velocities, no H I emission ($T_b < 0.1 \text{ K}$) is seen. Figures 1c and 1d show that the size of the emitting region generally becomes smaller as the velocity increases and that the region with enhanced emission is clumpy but evidently forms a shell structure. This velocity structure is an indication of an expanding shell. If we take $v_0 = +43 \text{ km s}^{-1}$ as the systematic velocity of W44 (Sato 1986), then Figures 1c and 1d imply the expansion velocity of $v_{\text{exp}} = 150 \pm 15 \text{ km s}^{-1}$. In principle, if the shell were symmetric, the approaching portion would be seen between $v_{\text{LSR}} = -110$ and -70 km s^{-1} . The absence of such HV H I emission implies that the shell is not symmetric. This asymmetry, however, seems to be a common property of expanding shells (Kulkarni & Heiles 1988).

Because of the confusion with the Galactic background H I emission, we cannot determine the size of the H I shell directly from our H I observations. Instead we multiply the mass-weighted average radius 7.5 of the shell at $v_{\text{LSR}} = +140 \text{ km s}^{-1}$ by $[1 - (v_{\text{LSR}} - v_0)^2/v_{\text{exp}}^2]^{-1/2} = 1.3$, which is the correction factor for the projection of a thin, uniformly expanding shell. Hence, the size of the H I shell is $\sim 10'$, or $R_H = 9 \text{ pc}$ if we use 3 kpc as a distance to W44.

The mass associated with the expanding H I shell at $v_{\text{LSR}} \geq +130 \text{ km s}^{-1}$ is $\Delta M = 73 \pm 3 M_{\odot}$ (including the cosmic abundance of helium). In order to derive the total mass of the expanding shell, we need to estimate the unobserved mass at lower velocities. In contrast to other SNRs for which the mass distribution as a function of line-of-sight velocity could be fitted by a Gaussian (Koo & Heiles 1991), the mass per unit line-of-sight velocity in W44 saturates at $v_{\text{LSR}} \lesssim +150 \text{ km s}^{-1}$. We simply multiply ΔM by 4.8, the ratio of the total velocity interval 300 km s^{-1} to the observed velocity interval 63 km s^{-1} to derive the total mass $M = 350 M_{\odot}$. The momentum and kinetic energy associated with the H I shell are $5 \times 10^4 M_{\odot} \text{ km s}^{-1}$ and $8 \times 10^{49} \text{ ergs}$, respectively. The derived physical parameters of the H I shell are summarized in Table 1. The large extrapolation factor makes the derived total mass in Table 1 very uncertain. On the other hand, if the energetic phenomena that produced the expanding H I shell had a spherical symmetry, it would have provided the momentum and kinetic energy comparable to those in Table 1.

4. DISCUSSION

4.1. Possibility of the Coincident H I and Radio Continuum Shells

The rapidly expanding H I shell that we have detected has a radius of $R_H = 9 \text{ pc}$, which is significantly smaller than $R_C = 13\text{--}17 \text{ pc}$ of the radio continuum shell. The radius R_H , however, is uncertain because it has been obtained by extrapolating the HV H I gas distribution. Therefore, we first consider the possibility that the two are located at the same distance from the center of W44 as in the ideal case of a SNR expanding into a uniform, homogeneous medium (e.g., Chevalier 1974; Tenorio-Tagle et al. 1990).

The presence of the H I shell suggests that the SNR is in the radiative phase. The age of the SNR is then $\sim 0.3 \bar{R}_C/v_{\text{exp}} = 2.9 \times 10^4 \text{ yr}$ (Cioffi, McKee, & Bertschinger 1988), where $\bar{R}_C = 15 \text{ pc}$ is the geometrical mean radius of the radio continuum shell. This age is not greatly different from the characteristic age $2 \times 10^4 \text{ yr}$ of the likely associated pulsar PSR 1853+01, so it is consistent with the radiative model. It is the centrally peaked *thermal* X-ray emission with large ($>0.2 \text{ cm}^{-3}$) electron density that is difficult to reconcile with the standard radiative model. For a SNR in a uniform medium, most of the hot gas is confined near the shock front, so that the SNR should appear as a shell type in X-ray. An old SNR could have a centrally peaked X-ray morphology either if the hot gas near the shock front is too cool to emit X-ray emission or if its X-ray emission, which is softer than that from the interior, is attenuated by relatively higher interstellar opacity at lower energies (SJWW; JSA). In the case of W44, however, the temperature of the X-ray-emitting gas is roughly uniform ($4\text{--}8 \times 10^6 \text{ K}$), and the electron density in the interior is large, which is not consistent with the standard SNR model (JSA; RPSH).

It has been suggested that a SNR expanding into a cloudy interstellar medium (ISM) is a plausible mechanism for the observed radio and X-ray morphology of W44 (SJWW; JSA; RPSH). The ISM is known to be composed of dense clouds immersed in a diffuse intercloud medium (Field, Goldsmith, & Habing 1969; McKee & Ostriker 1977). These dense clouds, once swept up by a SN blast wave, can deposit additional mass to the SNR through thermal evaporation. The density in the interior then becomes more or less uniform, and the X-ray emission would be centrally peaked (White & Long 1991). The radio emission would be still limb-brightened because of the shock propagating through the intercloud medium. But unfortunately this evaporative model does not explain the observed H I shell in W44 if it is coincident with the radio continuum shell. In order to explain the observed X-ray luminosity and its surface brightness, JSA and RPSH found that the intercloud density should be $0.06\text{--}0.26 \text{ cm}^{-3}$ depending on model parameters. This density is far too low to form a radiative dense shell of $350 M_{\odot}$ of radius 15 pc . Furthermore, the implied age is only $\sim 4000\text{--}7500 \text{ yr}$, which is much shorter than the characteristic age of PSR 1853+01.

The above considerations lead us to conclude that the H I and radio continuum shells are two physically distinct shells. According to our results, the H I shell is located well within the radio continuum shell. The SNRs expanding into a uniform, homogeneous medium cannot produce such a double-shell structure. If the ambient medium is uniform, but inhomogeneous, a similar structure seems to be possibly formed because the dense clouds initially close to the explosion center can be evacuated due to the ram pressure and cloud shock accelerations (McKee, Cowie, & Ostriker 1978; Tenorio-Tagle &

Różycka 1986; Różycka & Tenorio-Tagle 1987). The resulting spatial and velocity structures of the SNR in this case, however, depend on various physical parameters, and we need a detailed theoretical model in order to compare with our observations. In this paper, we consider an alternative model in which the ambient medium is homogeneous but not uniform.

4.2. W44 as a SNR Produced inside a Preexisting Wind Bubble

We propose that W44 is a SNR produced inside a preexisting wind bubble. W44 with PSR 1853+01 is believed to be a Type II (or Ib) SNR, and as such it is natural to assume that there was a preexisting diffuse wind bubble surrounded by a dense wind shell (WS). In the following, we show that the inner H I and the outer radio continuum structures may be interpreted as the WS and the SNR shell, respectively.

The evolution of a SNR in a preexisting wind bubble has been subject to some theoretical studies (Chevalier & Liang 1989, hereafter CL; Tenorio-Tagle et al. 1990, 1991). We first summarize the evolution based on these studies. The evolution of a SNR may be largely divided into three phases: (1) free expansion phase, (2) shell crossing phase, and (3) “memory-losing” phase. Detailed hydrodynamical properties of the flow in each phase depend on the density distributions of the SN ejecta and the ambient medium. We consider a SN ejecta with an outer steep power-law density distribution [$\rho(r) \propto r^{-k_{ej}}$] and inner flat density distribution (see CL). Tenorio-Tagle et al. carried out numerical simulations for $k_{ej} = 3$, which is close to the density distribution given by Woosley, Pinto, & Ensmann (1988). CL considered similarity solutions for $k_{ej} > 5$. According to Arnett’s (1988) numerical simulations for SN 1987A, k_{ej} is close to 9. The wind bubble is assumed to be filled with very diffuse uniform shocked wind. The free expansion phase is the period during which the blast wave propagates through the hot diffuse bubble. The expanding ejecta drives two shocks: a forward shock propagating into the shocked wind and a reverse shock propagating into the ejecta (in the ejecta’s reference frame). Both the shocked ejecta and the reshocked wind, separated by a contact discontinuity, are confined to a thin shell. Since the shell is decelerating and the shocked ejecta is denser than the reshocked wind on average, the contact discontinuity is subject to Rayleigh-Taylor (RT) instability. The development of RT instability has been shown beautifully in recent numerical simulations carried out by Chevalier, Blondin, & Emmering (1992). To the extent that only a small fraction of the ejecta experiences a shock, the evolution of the SNR at late phases would not depend on the detailed properties of the instability. In order for only a fraction of the SN ejecta in the power-law portion to be shocked before the blast wave hits the WS, the mass within the bubble M_1 should be smaller than $1.8\text{--}0.16M_{ej}$ (for $k_{ej} = 6\text{--}12$), where M_{ej} is the mass of the SN ejecta (CL). The more stringent criterion for larger k_{ej} arises because the fraction of the ejecta mass in the power-law portion is inversely proportional to k_{ej} , i.e., $\propto 3/k_{ej}$. For most wind bubbles, this criterion is likely to be satisfied (CL).

When the blast wave strikes the dense WS, the kinetic energy of the shocked wind is converted to thermal energy, and the postshock pressure increases by a factor of $\lesssim 6$ (Silk & Solinger 1973). The increased pressure drives two shocks: a transmitted shock which compresses the WS and a reflected shock which propagates back through the wind material and through the

SN ejecta. The reflected shock soon becomes a standing shock due to the increasing ram pressure of the incoming SN ejecta. The pressure in the interaction region, i.e., the region between the reflected shock and the transmitted shock, increases as $P_s \propto t^{k_{ej}-5}$ as far as the power-law portion of the SN ejecta interacts with the WS. The pressure stops rising and starts to decrease either (1) when all the SN ejecta in the power-law portion is shocked (τ_{bend}), (2) when the energy transferred to the WS becomes significant (τ_E), or (3) when the transmitted shock crosses the WS (τ_{cross}). If the reflected shock is adiabatic with the adiabatic index of $\gamma = 5/3$ and the transmitted shock is radiative ($\gamma = 1$), then the three time scales are given by (from CL)²

$$\tau_{bend} = \left[\frac{432(k_{ej} - 3)^3}{125(k_{ej} - 5)(4k_{ej} - 15)^2} \right]^{1/6} \frac{R_1}{v_{ej}}, \quad (1a)$$

$$\tau_E = \left[\frac{25(3k_{ej} - 13)^2}{16(k_{ej} - 3)^2(4k_{ej} - 15)^2} \left(\frac{\Delta R_1}{R_1} \right)^{-2} \right]^{1/(k_{ej}-3)} \tau_{cross} \quad (1b)$$

and

$$\tau_{cross} = \left[\frac{4(k_{ej} - 5)}{4k_{ej} - 15} \right]^{1/[3(k_{ej}-3)]} \times \left[\frac{5k_{ej}(k_{ej} - 4)}{24} \left(\frac{M_{ws}}{M_{ej}} \right) \left(\frac{\Delta R_1}{R_1} \right) \right]^{1/(k_{ej}-3)} \tau_{bend}, \quad (1c)$$

and where $v_{ej} \equiv (2E/M_{ej})^{1/2}$ is the characteristic velocity of the ejecta (with the SN explosion energy $E = 10^{51}$ ergs) and ΔR_1 , R_1 , and M_{ws} are the thickness, radius, and mass of the WS, respectively. We have obtained equation (1b) and (c) by assuming that all the mass initially inside R_1 is contained in the WS.

The late morphology of a SNR is largely determined in this shell crossing phase. If the transmitted shock can cross the WS and propagate into the undisturbed ISM, then the SNR would have a double shell structure. On the other hand, if it merges into the WS, the SNR will have only a single shell structure (see below). According to above discussions, the blast wave can cross the WS while the power-law portion of the SN ejecta is interacting with the WS if τ_{cross} is shorter than τ_E and τ_{bend} . Using equations (1a)–(1c), the condition $\tau_{cross} < \tau_E$ requires

$$\Delta R_1/R_1 < 0.23\text{--}0.097, \quad (k_{ej} = 6\text{--}12), \quad (2)$$

whereas the condition $\tau_{cross} < \tau_{bend}$ requires

$$\frac{M_{ws}}{M_{ej}} < 5.2\text{--}0.53 \left(\frac{\Delta R_1/R_1}{0.1} \right)^{-1}, \quad (k_{ej} = 6\text{--}12). \quad (3)$$

Hence, if the WS is thin and its mass is relatively small, then the double-shell structure is expected. However, it should be noted that these conditions are sufficient but *not* necessary for the double-shell structure. The blast wave can still cross the shell while the flat portion of the SN ejecta is interacting with the WS, although the driving pressure decreases because the

² There are some typographical errors in the paper of CL. The numerical factor “3” in denominator of their eq. (3.15) should be read as “4,” whereas the factor “ $\gamma - 1$ ” in the numerator of the first term in eq. (3.16) should be read as “ $\gamma + 1$.” Also, the exponent “ $(n + 1)/3$ ” in eq. (3.24) should be read as “ $(n + 4)/3$.”

TABLE 2
PARAMETERS OF THE SNR W44

Parameter	Estimated Value
Age	2×10^4 yr
Wind Shell:	
Initial radius	7.5 pc
Current radius	9 pc
Expansion velocity	150 km s^{-1}
SNR Shell:	
Radius	15 pc
Expansion velocity	330 km s^{-1}

reverse shock propagates toward the center. In order to derive the necessary conditions for the double-shell structure, we need a careful analysis of the shell crossing phase which is beyond the scope of this paper. For $k_{ej} = 3$, Tenorio-Tagle et al. (1991) concluded that M_{ws}/M_{ej} should be less than ~ 50 for the double-shell structure.

In practice, however, even the massive WSs are likely to have the double-shell structure for the following reasons. First, since the WS accelerates while interacting with the power-law portion of the SN ejecta, the WS is subject to RT instability. The two-dimensional numerical simulations by Tenorio-Tagle et al. (1991) show the developing RT tongues, although since $k_{ej} = 3$ in their case, the instability might have developed during the initial interaction. For $k_{ej} > 7$, the acceleration increases with time, and the RT instability might disrupt the shell more effectively. Second, the SN ejecta may be fragmented, in which case the fragments can punch holes in the WSs (Tenorio-Tagle et al. 1991). In either case, the WS is expected to be disrupted, so that the hot gas is able to pass through the WS to drive a new shock in the undisturbed ISM. The new shock will produce an outer SNR shell, which will approach the standard model once the swept-up mass of the ambient gas becomes comparable to the mass of the WS.

We call this final phase the “memory-losing” phase, because the SN blast wave has now obliterated the presence of the wind bubble. A SNR in the memory-losing phase will have a double-shell structure. The outer SNR shell is likely to be evolving as a standard SNR, while the inner WS is likely to be coasting at a constant velocity acquired at the end of disruption. Most of the volume in the interior of the WS is to be filled with shocked SN ejecta.

According to the above discussion, W44 is considered to be in the memory-losing phase. The outer SNR shell appears only in radio continuum, presumably because it is in the Sedov phase. The inner WS appears in the H I 21 cm line and in optical emission because the shock is radiative. The fragmented HV H I shell suggests a disrupted WS. The centrally brightened X-ray emission is likely due to the SN ejecta filling the interior of the WS and also partly due to the material evaporated from the WS. As we will show next, the X-ray emission from the outer SNR shell is too soft to be detected. Hence, the observed morphology of W44 seems to be consistent with a SNR produced by the SN explosion inside a preexisting wind bubble.

4.3. Parameters of the SNR W44

Let us now derive some physical parameters of W44. If the H I shell was initially at R_1 and started to coast with its current

velocity v_{exp} at t_1 , then its age is

$$t_H = t_1 + \frac{R_H}{v_{exp}} \left(1 - \frac{R_1}{R_H} \right). \quad (4)$$

This age should be identical to the age of the radio continuum shell. We assume that the radio continuum shell is in the Sedov phase. However, there is a difficulty in assuming a uniform density distribution for the initial ambient medium. Because the mass of the H I shell is $350 M_\odot$, the mean density of the initial ambient medium must be greater than 3.3 cm^{-3} . If the initial size of the WS was, say, 20% smaller than R_H , the mean density would be 5.8 cm^{-3} . Then the age of the radio continuum shell, assuming the Sedov solution, is 3.8×10^4 yr, and its current expansion velocity is 160 km s^{-1} . This age is significantly greater than the characteristic age of PSR 1853+01, which implies that a second rapidly expanding H I shell should be associated with the radio continuum shell—which is not observed.

We therefore consider an initial ambient ISM with a power-law density distribution, $\rho_a(r) \propto r^{-k_a}$. Molecular clouds generally have $k_a = 1$ –1.3 (Cernicharo, Bachiller, & Duvert 1985; Stüwe 1990). For a Sedov SNR in this power-law density distribution, the age is given by

$$t_c = 1260 \xi^{-1/2} R_1^{(2-k_a)/2} \left(\frac{R_c}{R_1} \right)^{(5-k_a)/2} \text{ yr}, \quad (5)$$

where ξ is a constant of order of unity that depends on k_a , and R_1 and R_c are in parsecs (see Ostriker & McKee 1988). In order for both t_H and t_c to be consistent with the characteristic age of PSR 1853+01, we find that k_a should be in a narrow range, $0.4 \lesssim k_a \lesssim 0.6$. For the purpose of a numerical estimate, we take $k_a = 0.5$, which yields $t_1 = 1.0 \times 10^4$ yr, $R_1 = 7.5$ pc and the current expansion velocity $v_c = 330 \text{ km s}^{-1}$. The derived parameters of W44 are summarized in Table 2. Note that the expansion velocity of the SNR shell is significantly different from previous estimates. JSA and RPSH, using the evaporative SNR model of White & Long (1991), have derived an age of $t = 4000$ –7500 yr, which implies an expansion velocity of $v_c = 2\bar{R}_c/5t = 780$ –1500 km s^{-1} . The large expansion velocity is because, in the evaporative model, the postshock temperature is greater (by a factor of 1.4–3.6 for $C/\tau = 3$ –5) than the observed X-ray temperature (4 – 8×10^6 K).

For a SNR in the Sedov phase, the volume-averaged mean pressure inside the SNR is $\bar{P}/k_B = 0.106E/(k_B R_c^3) = 7.8 \times 10^6 \text{ cm}^{-3} \text{ K}$ (for $k_a = 0.5$; Ostriker & McKee 1988), where k_B is the Boltzmann constant. The pressure within W44, including the region inside the WS, should be close to this. According to SJWW, the electron density and the temperature in the central X-ray-emitting region are 0.5 cm^{-3} and 10^7 K, which yield a pressure consistent with the above. On the other hand, the implied postshock temperature and density are 1.6×10^6 K and 4 cm^{-3} . These numbers are consistent with the limits imposed by the low X-ray surface brightness of the shell (SJWW).

5. CONCLUSIONS

We have shown that the observed morphology of W44 at various wavelengths indicates that it is an old ($\sim 2 \times 10^4$ yr) SNR produced by a SN explosion inside a preexisting wind cavity. Although there has been previous evidence for the existence of presupernova cavities (see Franco et al. 1991), W44 is

the first SNR that is old enough to show a well-separated double-shell structure. It is particularly interesting that the inner H I shell, which is presumably the preexisting wind shell, shows highly fragmented structure as expected from theoretical considerations. The degree of fragmentation is probably related to the steepness of the density distribution of the SN ejecta, which needs a detailed theoretical study for comparison. High-resolution H I 21 cm line observations for other shell-type SNRs with high-velocity H I gas (Koo & Heiles 1991) could reveal more examples of such *memory-losing* SNRs.

We wish to thank the referee, Namir Kassim, for comments which improved the presentation of this paper. We thank Wolfgang Reich for providing us with the Bonn 11 cm survey data. We also thank Roger Chevalier and Guillermo Tenorio-Tagle for their helpful comments. B.-C. K. would like to thank the Center for Astrophysics for its hospitality and financial support during a portion of this research. This work has been supported in part by the 1994 KOSEF International Cooperative Research Fund.

REFERENCES

- Arnett, W. D. 1988, *ApJ*, 331, 377
 Braun, R., & Strom, R. G. 1987, *A&A*, 164, 193
 Castor, J., McCray, R., & Weaver, R. 1975, *ApJ*, 200, L107
 Caswell, J. L., Murray, J. D., Roger, R. S., Cole, D. J., & Cooke, D. J. 1975, *A&A*, 45, 239
 Cernicharo, J., Bachiller, R., & Durvert, G. 1985, *A&A*, 149, 273
 Chevalier, R. A. 1974, *ApJ*, 188, 501
 Chevalier, R. A., Blondin, J. M., & Emmering, R. T. 1992, *ApJ*, 392, 118
 Chevalier, R. A., & Liang, E. P. 1989, *ApJ*, 344, 332 (CL)
 Cioffi, D. F., McKee, C. F., & Bertschinger, E. 1988, *ApJ*, 334, 252
 Clark, D. A., Green, A. J., & Caswell, J. L. 1975, *Australian J. Phys., Astrophysical Suppl.*, No. 37, 1
 Field, G. B., Goldsmith, D., & Habing, H. 1969, *ApJ*, 15, L49
 Franco, J., Tenorio-Tagle, G., Bodenheimer, P., & Różyczka, M. 1991, *PASP*, 103, 803
 Jones, L. R., Smith, A., & Angellini, L. 1993, *MNRAS*, 265, 631 (JSA)
 Kassim, N. E. 1992, *AJ*, 103, 943
 Koo, B.-C., & Heiles, C. 1991, *ApJ*, 382, 204
 Kulkarni, S. R., & Heiles, C. 1988, in *Galactic and Extragalactic Radio Astronomy*, ed. G. L. Verschuur & K. I. Kellermann (New York: Springer), 95
 Kundu, M. R., & Velusamy, T. 1972, *A&A*, 20, 237
 Long, K. S., Blair, W. P., White, R. L., & Matsui, Y. 1991, *ApJ*, 373, 567
 McKee, C. F., Cowie, L. L., & Ostriker, J. P. 1978, *ApJ*, 219, L23
 McKee, C. F., & Ostriker, J. P. 1977, *ApJ*, 217, 148
 Ostriker, J. P., & McKee, C. F. 1988, *Rev. Mod. Phys.*, 60, 1
 Reich, W., Fürst, E., Reich, P., & Reif, K. 1990, *A&AS*, 85, 633
 Rho, J.-H., Petre, R., Schlegel, E. M., & Hester, J. J. 1994, *ApJ*, 430, 757 (RPSH)
 Różyczka, M., & Tenorio-Tagle, G. 1987, *A&A*, 176, 329
 Sato, F. 1986, *AJ*, 91, 378
 Silk, J., & Solinger, A. 1973, *Nature Phys. Sci.*, 244, 101
 Smith, A., Jones, L. R., Watson, M. G., & Willingale, R. 1985, *MNRAS*, 217, 99 (SJWW)
 Stüwe, J. A. 1990, *A&A*, 237, 178
 Tenorio-Tagle, G., Bodenheimer, P., Franco, J., & Różyczka, M. 1990, *MNRAS*, 244, 563
 Tenorio-Tagle, G., & Różyczka, M. 1986, *A&A*, 155, 120
 Tenorio-Tagle, G., Różyczka, M., Franco, J., & Bodenheimer, P. 1991, *MNRAS*, 251, 318
 Weaver, R., McCray, R., Castor, J., Shapiro, P., & Moore, R. 1977, *ApJ*, 218, 377
 White, R. L., & Long, K. S. 1991, *ApJ*, 373, 545
 Wolszczan, A., Cordes, J. M., & Dewey, R. J. 1991, *ApJ*, 372, L99
 Woosley, S. E., Pinto, P. A., & Ensman, L. 1988, *ApJ*, 324, 466